29. Harris TR, Overholser KA, Stiles RG. Concurrent increases in resistance and transport after coronary obstruction in dogs. *Am J Physiol* 1981;240(*Heart Circ Physiol* 9):H262–H273.
30. Yipintsoi T, Dobbs WA Jr, Scanlon PD, Knopp TJ, Bassingthwaighte JB. Regional distribution of diffusible tracers and carbonized microspheres in the left ventricle of isolated dog hearts. *Circ Res* 1973;33:573–587.
31. Goresky CA, Bach GG, Nadeau BE. Red cell carriage of label: its limiting effect on the exchange of materials in the liver. *Circ Res* 1975;36:328–351.
32. Bergmann SR, Hack SN, Sobel BE. "Redistribution" of myocardial thallium-201 without reperfusion: Implications regarding absolute quantification of perfusion. *Am J Cardiol* 1982;49:1691–1698.
33. Weich HF, Strauss HW, Pitt B. The extraction of thallium-201 by the myocardium. *Circulation* 1977;56:188–191.
34. Martin P, Yudilevich DL. A theory for the quantification of transcapillary exchange by tracer-dilution curves. *Am J Physiol* 1964;207:162–168.
35. Bassingthwaighte JB, Ackerman FH, Wood EH. Applications of the lagged normal density curve as a model for arterial dilution curves. *Circ Res* 1966;18:398–415.
36. Chan IS, Goldstein AA, Bassingthwaite JB. SENSOP: a derivative-free solver for nonlinear least squares with sensitivity scaling. *Ann Biomed Eng* 1993;21:621–631.
37. Curry FE, Michel CC. A fiber matrix model of capillary permeability. *Microvasc Res* 1980;20:96–99.
38. L'Abbate A, Biagini A, Michelassi C, Maseri A. Myocardial kinetics of thallium and potassium in man. *Circulation* 1979;60:776–785.
39. Alvarez OA, Yudilevich DL. Heart capillary permeability to lipid-insoluble molecules. *J Physiol* 1969;202:45–58.
40. Durán WN, Yudilevich DL. Estimate of capillary permeability coefficients of canine heart to sodium and glucose. *Microvasc Res* 1978;15:195–205.
41. Roselli RJ, Harris TR. A four-phase model of capillary tracer exchange. *Ann Biomed Eng* 1979;7:203–238.
42. Hille B. The permeability of the sodium channel to metal cations in myelinated nerve. *J Gen Physiol* 1972;59:637–658.
43. Hougen TJ, Smith TW. Inhibition of myocardial monovalent cation active transport by subtoxic doses of ouabain in the dog. *Circ Res* 1978;42:856–863.
44. Hougen TJ, Lloyd BL, Smith TW. Effects of inotropic and arrhythmogenic digoxin doses and of digoxin-specific antibody on myocardial monovalent cation transport in the dog. *Circ Res* 1979;44:23–31.
45. Winkler B, Schaper W. Tracer kinetics of thallium, a radionuclide used for cardiac imaging. In: Schaper W, ed. *The pathophysiology of myocardial perfusion*. Amsterdam: Elsevier/North Holland: 1979:102–112.
46. Dani JA, Levitt DG. Water transport and ion-water interaction in the gramicidin channel. *Biophys J* 1981;35:501–508.
47. Reuter H, Stevens CF. Ion conductance and ion selectivity of potassium channels in snail neurones. *J Membrane Biol* 1980;57:103–118.
48. Winkler B, Schaper W. The role of radionuclides for cardiac research. In: Pabst HW, Adam WE, Ell P, Hör G, Kriegel H, eds. *Handbook of nuclear medicine*, vol. 2: *Heart*. Stuttgart, New York: Gustav Fischer; 1992:390–407.
49. Krivokapich J, Watanabe CR, Shine KI. Effects of anoxia and ischemia on thallium exchange in rabbit myocardium. *Am J Physiol* 1985;249:H620–H628.
50. Grunwald AM, Watson DD, Holzgrefe HH Jr, Irving JF, Beller GA. Myocardial thallium-201 kinetics in normal and ischemic myocardium. *Circulation* 1981;64:610–618.
51. Budinger TF, Yano Y, Huesman RH, et al. Positron emission tomography of the heart. *Physiologist* 1983;26:31–34.
52. Nielsen AP, Morris KG, Murdock R, Bruno FP, Cobb FR. Linear relationship between the distribution of thallium-201 and blood flow in ischemic and nonischemic myocardium during exercise. *Circulation* 1980;61:797–801.
53. Pohost GM, Okada RD, O'Keefe DD, et al. Thallium redistribution in dogs with severe coronary artery stenosis of fixed caliber. *Circ Res* 1981;48:439–446.
54. Cousineau DF, Goresky CA, Rose CP, Simard A, Schwab AJ. Effects of flow, perfusion pressure, and oxygen consumption on cardiac capillary exchange. *J Appl Physiol* 1995;78:1350–1359.
55. Okada RD, Leppo JA, Strauss HW, Boucher CA, Pohost GM. Mechanisms and time course for the disappearance of thallium-201 defects at rest in dogs. *Am J Cardiol* 1982;49:699–706.
56. Okada RD, Jacobs ML, Daggett WM, et al. Thallium-201 kinetics in nonischemic canine myocardium. *Circulation* 1982;65:70–77.
57. Leppo JA, Meerdink DJ. A comparison of the myocardial uptake of a technetium-labeled isonitrile analog and thallium. *Circ Res* 1989;65:632–639.
58. Leppo JA, Meerdink DJ. Comparative myocardial extraction of two technetium-labeled BATO derivatives (SQ30217, SQ32014) and thallium. *J Nucl Med* 1990;31:67–74.
59. Maublant JC, Gachon P, Moins N. Hexakis (2-methoxy isobutylisonitrile) technetium-99m and thallium-201-chloride: uptake and release in cultured myocardial cells. *J Nucl Med* 1988;29:48–54.
60. Marcus ML, Kerber RE, Erhardt JC, Falsetti HL, Davis DM, Abboud FM. Spatial and temporal heterogeneity of left ventricular perfusion in awake dogs. *Am Heart J* 1977;94:748–754.
61. King RB, Bassingthwaighte JB, Hales JRS, Rowell LB. Stability of heterogeneity of myocardial blood flow in normal awake baboons. *Circ Res* 1985;57:285–295.
62. Bassingthwaighte JB, Malone MA, Moffett TC, et al. Molecular and particulate depositions for regional myocardial flows in sheep. *Circ Res* 1990;66:1328–1344.
63. Crank J. *The mathematics of diffusion*. Oxford: Clarendon Press; 1956.
64. Pollock F, Blum JJ. On the distribution of a permeable solute during Poiseuille flow in capillary tubes. *Biophys J* 1966;6:19–29.
65. Aroesty J, Gross JF. Convection and diffusion in the microcirculation. *Microvasc Res* 1970;2:247–267.
66. Gonzalez-Fernandez JM, Atta SE. Concentration of oxygen around capillaries in polygonal regions of supply. *Math Biosci* 1972;13:55–69.

Kinetics of Technetium-99m-Teboroxime in Reperfused Nonviable Myocardium

Robert D. Okada, David K. Glover, Jeffrey D. Moffett, Delia Beju and Gerald Johnson III
William K. Warren Medical Research Institute, University of Oklahoma Health Sciences Center, Tulsa, Oklahoma

This study evaluates ^{99m}Tc-teboroxime uptake and clearance kinetics in reperfused infarcted myocardium. **Methods:** In 47 isolated buffer perfused rat hearts, 17 had normal flow (Control), 13 had 30 min of no flow followed by reflow (Noflow30) and 11 had 60 min of no flow followed by reflow (Noflow60). A 1-hr uptake phase was begun by normally perfusing all 41 hearts with ^{99m}Tc-teboroxime-doped buffer. After uptake, a 1-hr clearance phase was begun by switching to a ^{99m}Tc-teboroxime-free buffer. Technetium-99m activity was monitored with a NaI probe. Triton X-100, a membrane detergent, was given after tracer loading to six additional hearts. **Results:** Control and Noflow30 hearts showed near linear and rapid uptake, while Noflow60 hearts showed curvilinear and significantly less uptake than predicted. All three of these groups showed biexponential clearance. Early $t_{1/2}$ was not significantly different for the three groups (Control = 6.3 ± 1.9 sem min, Noflow30 = 5.4 ± 1.3 min, Noflow60 = 8.9 ± 2.8 min). Late $t_{1/2}$ was significantly shorter for Noflow30 (52.3 ± 5.3 min) and the Noflow60 (50.9 ± 4.3 min), compared to the Control hearts (74.1 ± 6.6 min, $p < 0.05$). One-hour fractional clearances were significantly greater for the Noflow30 and Noflow60 hearts (0.65 ± 0.01 and 0.65 ± 0.01, respectively) compared to the Controls (0.55 ± 0.01, $p < 0.05$). In hearts given Triton X-100, there was a markedly increased fractional clearance of 0.96 ± 0.01 ($p < 0.01$ compared to Controls). Electron microscopy showed evidence of mild injury in the Noflow30 hearts, more extensive damage in the Noflow60 hearts and severe irreversible injury in Triton X-100 hearts. **Conclusion:** Myocardial ^{99m}Tc-teboroxime uptake and clearance kinetics are significantly altered in mildly and moderately injured reperfused myocardium. Technetium-99m-teboroxime clearance is markedly accelerated in the setting of overt damage to cell and organelle membranes induced by Triton X-100.

Key Words: technetium-99m-teboroxime; kinetics; reperfused; nonviable; myocardium

J Nucl Med 1997; 38:274–279

Received Dec. 27, 1995; revision accepted June 13, 1996.

For correspondence or reprints contact: Gerald Johnson III, PhD, William K. Warren Medical Research Institute, 6465 South Yale, Suite 1010, Tulsa, OK 74136-7862.

Technetium-99m-teboroxime is a myocardial imaging agent that has 90% first-pass extraction (*1*), uptake that increases linearly with flow (*2–4*) and clearance that decreases with decreased flow in viable myocardium (*5–10*). Because ^{99m}Tc-teboroxime is potentially a better flow marker than thallium or sestamibi, its use has been proposed to assess reperfusion after thrombolytic therapy (*2,11*). However, the uptake and clearance kinetics of ^{99m}Tc-teboroxime in reperfused nonviable myocardium have not been thoroughly reported. This study investigates these kinetics in a perfused rat heart model of acute myocardial infarction followed by reperfusion and in a model of cell lysis induced by Triton X-100. We postulated that metabolic and structural abnormalities created by infarction and reperfusion injury would affect ^{99m}Tc-teboroxime myocardial uptake and clearance kinetics despite normalization of flow.

MATERIALS AND METHODS

Isolated, Perfused Heart Preparation

Male Sprague-Dawley rats (weighing 375 to 400 g) were anesthetized with 65 mg intraperitoneal sodium pentobarbital. After deep anesthesia was achieved, 400 units heparin were administered intravenously and the heart was removed through a rapid parasternal thoracotomy. The heart was then immediately placed in modified Krebs-Henseleit buffer at 4°C. The aortic stump was then attached by suture to the cannula of the perfusion apparatus which is shown in Figure 1. A Masterflex pump (Parmer Instruments, Burlington, IL) controlled the perfusion rate of the buffer and removed sinus drainage. Flow was held constant at 12 ml/min without recirculation. Temperature of the perfusate was maintained at 37°C by a water bath.

All hearts were retrogradely perfused using a modified Krebs-Henseleit buffer containing (mmol/liter): 1.25 KH2PO4, 0.56 MgSO4, 1.51 CaCl2, 4.88 KCl, 0.833 EDTA, 127 NaCl, 20 NaHCO3 and 5.77 pyruvate. This buffer was continuously bubbled with 95% O_2/5%CO_2 and maintained at pH 7.4 ± 0.05 and O_2 > 300% saturation. Triton X-100 perfusate was prepared by adding 100% Triton X-100 to the Krebs-Henseleit buffer to make a 0.5% solution of Triton X-100 by volume.

A small saline-filled, latex balloon-tipped catheter was passed through a slit in the left atrial appendage and into the left ventricle. The balloon was inflated to achieve a pressure of 100 mmHg throughout the experiment. Pressure was measured by a Statham p23d pressure transducer connected to the left ventricular catheter. All hearts were atrially paced (Model 5320, Medtronic, Minneapolis, MN) at 300 bpm. This constant work load preparation was used since functional data was not felt to be relevant in this model. Temperature and oxygen saturation of the perfusate were monitored online by a probe. The pH was monitored by a separate inline probe. Left ventricular pressure, temperature, pH and oxygen levels were continuously recorded on a physiological recorder.

As shown in Figure 1, two buffer storage tanks were filled with 1 liter of the Krebs-Henseleit buffer. The uptake phase tank was doped with 500 μCi ^{99m}Tc-teboroxime, whereas the clearance and control tank was nonradioactive. The buffer storage and waste area was shielded from the measurement area by lead walls. An IBM PC-AT computer was used to switch between the radioactive uptake and the nonradioactive clearance buffers at the appropriate time by controlling solenoid valves. The computer also controlled the perfusion rate of the Masterflex pump used to deliver the buffer and remove the sinus drainage. Myocardial ^{99m}Tc-teboroxime activity was monitored at 1-min intervals using a lead collimated sodium iodide scintillation detector placed in close proximity to the heart. Time-activity curves were recorded for each experiment. These curves were displayed on a computerized multichannel analyzer. Myocardial clearance curves were corrected for background and decay.

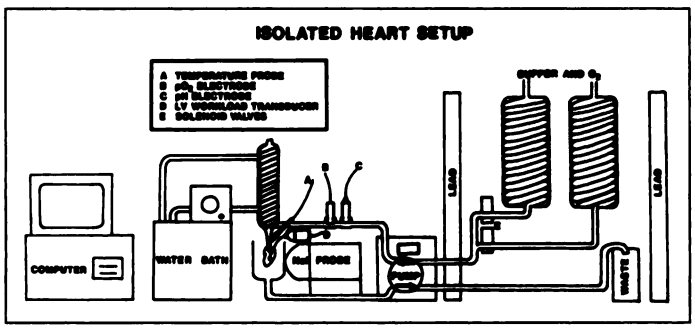

FIGURE 1. Isolated buffer perfused rat heart apparatus.

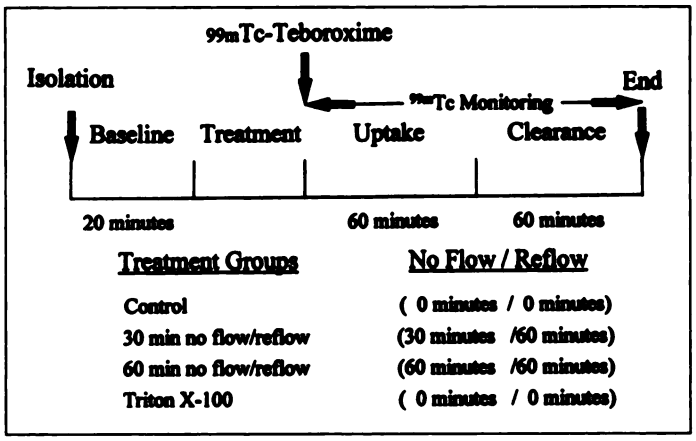

FIGURE 2. Experimental protocol.

Technetium-99m-Teboroxime Preparation

Kits for the preparation of ^{99m}Tc-teboroxime were supplied in a lyophilized form by Squibb Diagnostics, Princeton, NJ. A vial of ^{99m}Tc-teboroxime was reconstituted by addition of 25 mCi of ^{99m}Tc-pertechnetate. The vial was then heated for 15 min to 100°C using a heating block. After cooling to room temperature, paper chromatography was performed to determine the percentage of soluble contaminants and reduced hydrolyzed technetium. Whatman 31 ET chromatography strips (1.3 × 11 cm) and two individual mobile-phase solvent systems were used to determine the radiochemical purity of the prepared product. The developed chromatographs were air-dried and counted. The results indicated that radiochemical purity was 94.0 ± 0.4%. The compound was stored at room temperature until used, which was within 6 hr of preparation.

Electron Microscopy

Ultrastructural injury was assessed by transmission electron microscopy. At the end of the experiment, two hearts from each group were perfused with 2% glutaraldehyde in 0.1 *M* cacodylate buffer at pH 7.4. The hearts were postfixed in 1% osmium tetroxide, en bloc stained with 0.5% aqueous uranyl acetate, dehydrated in graded ethanol and embedded in PolyBed 812. Thin sections were obtained with MT-6000 and MT-2B ultramicrotomes equipped with diamond knives. The sections were contrasted with uranyl acetate and lead citrate and were examined in a Zeiss 109 electron microscope operated at 80 kV.

Experimental Protocol

In 47 experiments, rat hearts were isolated, mounted on the perfusion apparatus and perfused at 12 ml/min for 20 min to ensure stabilization (Fig. 2). In 17 control hearts, normal flow rates were continued for an additional 30 min; in 13 hearts, flow was completely shut off for 30 min before resuming normal flow (30 min no flow/reflow group); and in 11 hearts, flow was completely

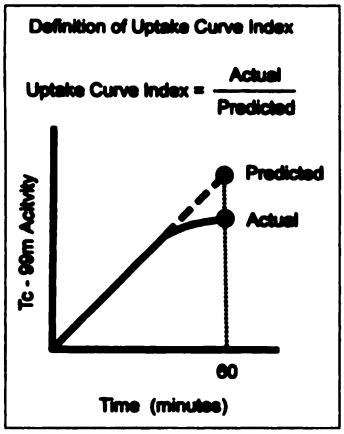

FIGURE 3. Schematic diagram of method for calculating uptake curve index.

shut off for 60 min before resuming normal flow (60 min no flow/reflow group). Next, a 1-hr ^{99m}Tc-teboroxime uptake phase was begun by switching to the radioactive buffer tank perfused at 12 ml/min for 60 min. At the end of the 60-min uptake phase, a 1-hr clearance phase was begun by switching to the nonradioactive buffer at 12 ml/min. Technetium-99m-teboroxime activity was monitored throughout the 120-min period after tracer administration.

In six additional hearts given Triton X-100, a protocol similar to the control hearts was used. Triton X-100 is a nonionic detergent which lyses cell membranes. Technetium-99m-teboroxime was administered during control conditions, since little uptake would have occurred after Triton X-100 treatment. However, during the clearance phase, hearts were perfused with Krebs-Henseleit buffer containing 0.5% Triton X-100 at 12 ml/min.

Data Analysis

For each individual heart, background counts taken for 5 min before the ^{99m}Tc-teboroxime uptake phase were averaged and subtracted from the activity recorded on the multichannel analyzer for each minute of clearance. The background-subtracted counts were then corrected for ^{99m}Tc decay. The background-subtracted, decay-corrected counts were then used to calculate fractional ^{99m}Tc-teboroxime washout. Time-activity curves were normalized as a percentage of peak uptake. Data from individual experiments also were averaged to obtain mean curves for each group.

To quantitatively compare the shape of the ^{99m}Tc-teboroxime uptake curves, an uptake curve index was calculated (Fig. 3). The uptake curve index was the ratio between the actual peak myocardial uptake and the peak myocardial uptake predicted from linear regression analysis of the uptake curve. Thus, an uptake curve index less than 1.0 would indicate a plateauing of the uptake curve.

Curve-Fitting Technique

Nonlinear regression analysis was used to fit clearance curve data by means of automated curve-fitting software using a Levenburg-Marquardt least squares algorithm (TableCurve 2D, Jandel Scientific, San Rafael, CA). The best fit statistic used was the r^2 value.

Statistical Analysis

One-way analysis of variance (ANOVA) procedure (Crunch Statistical Software, San Diego, CA) was used to analyze group differences. When the assumption of homogeneity of variance among groups was violated, the equivalent nonparametric (Kruskal-Wallis) analysis was used. Tests of mean differences were conducted by analysis with t-tests using the Bonferroni correction for multiple tests. A difference was considered to be statistically significant if $p < 0.05$. Data were reported as mean ± s.e.m.

TABLE 1
Myocardial Teboroxime Uptake and Clearance Parameters

Group	Fractional clearance	Uptake curve index	Early $t_{1/2}$	Late $t_{1/2}$
Control (n = 17)	0.55 ± 0.01	1.2 ± 0.05	6.3 ± 1.9	74.1 ± 6.6
Noflow30 (n = 13)	0.65 ± 0.01*	1.2 ± 0.07	5.4 ± 1.3	52.3 ± 5.3*
Noflow60 (n = 11)	0.65 ± 0.01*	0.9 ± 0.05*	8.9 ± 2.8	50.9 ± 4.3*
Triton X-100 (n = 6)	0.96 ± 0.01*	1.2 ± 0.05	2.0 ± 0.2*	20.1 ± 0.8*

Mean ± s.e.m.; *$p < 0.05$ compared to control; $t_{1/2}$ = time to reach one-half initial activity; early = first exponent in biexponential nonlinear curve fit; late = second exponent in biexponential nonlinear curve fit; Noflow30 = 30-min no flow/reflow group; Noflow60 = 60-min no flow/reflow group.

Ethics

All experimental animals were handled in accordance with the Position of the American Heart Association on Research Animal Use and the approval of the Institutional Animal Care and Use Committee of the University of Oklahoma Health Sciences Center.

RESULTS

General

The left ventricular balloon pressure was maintained at 100 mmHg, and the hearts were paced at 300 bpm throughout the experiments. Visually, contractility ceased during no flow and resumed after reflow in all experiments.

Myocardial Uptake

Table 1 lists the myocardial ^{99m}Tc-teboroxime uptake curve indices for the four groups. Normal control hearts demonstrated near linear and rapid myocardial ^{99m}Tc-teboroxime uptake, with a curve index near unity (1.16 ± 0.05). The 30-min no flow/reflow group also demonstrated near linear and rapid uptake, with a curve index identical to control (1.16 ± 0.06, p = ns). However, the 60-min no flow/reflow group demonstrated a curvilinear uptake, with a curve index of 0.90 ± 0.05 ($p < 0.05$ compared to control and 30 min no flow/reflow). The Triton X-100 hearts demonstrated a curve index similar to the control group, since ^{99m}Tc-teboroxime was administered to the group during control conditions.

Figure 4 demonstrates the group mean myocardial uptake curves for the first 5 min after the onset of the infusion. These first 5 min were felt to be most relevant to a bolus injection in patients. At 5 min, uptake was significantly greater for the control and the 30 min no flow/reflow group compared to the 60 min no flow/reflow group ($p < 0.05$). Triton X-100 hearts demonstrate an uptake curve similar to that of controls.

Myocardial Clearance

Figure 5 demonstrates the mean myocardial ^{99m}Tc-teboroxime clearance curves for the control, 30-min no flow/reflow, 60-min no flow/reflow and Triton X-100 groups. All four groups demonstrated a biphasic clearance pattern. Myocardial retention was less for the 30-min no flow/reflow and the 60-min no flow/reflow groups compared to control at every time point ($p < 0.01$). The Triton X-100 hearts demonstrated an even lower retention at every time point compared to the other three groups ($p < 0.01$).

When modeled, all four groups demonstrated a biexponential clearance (Table 1). Early $t_{1/2}$ was not significantly different for

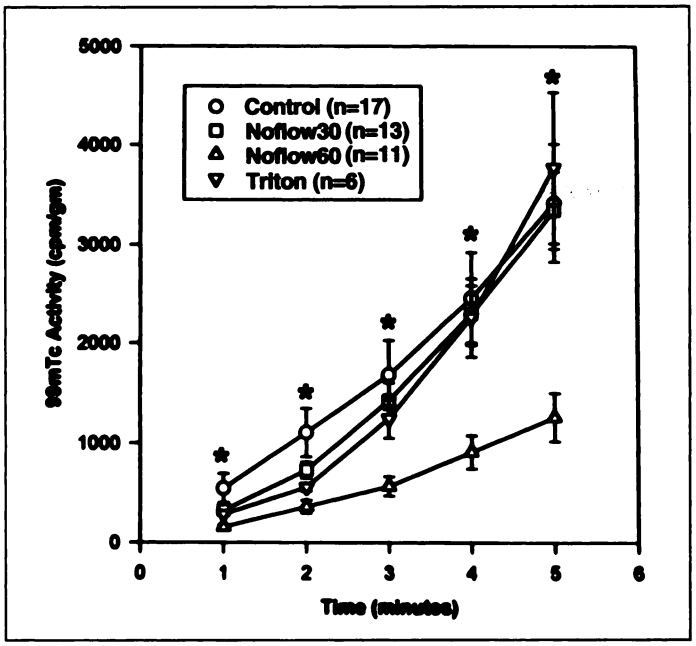

FIGURE 4. Mean decay and background-corrected ^{99m}Tc-teboroxime myocardial uptake curves for the four groups. *p < 0.05 from Noflow60.

the control (6.3 ± 1.9 min.), 30-min no flow/reflow (5.4 ± 1.3 min) and 60-min no flow/reflow groups (8.9 ± 2.8 min., p = ns). Triton X-100 hearts, however, demonstrated a significantly shorter early $t_{1/2}$ (2.0 ± 0.2 min, p < 0.05) compared to controls. Late $t_{1/2}$ was significantly shorter for the 30-min no flow/reflow group (52.3 ± 5.3 min.) and the 60-min no flow/reflow group (50.9 ± 4.3 min.) compared to controls (74.1 ± 6.6 min., p < 0.05). Triton X-100 hearts demonstrated an even shorter late $t_{1/2}$ (20.1 ± 0.8 min., p < 0.05) compared to other groups.

Table 1 demonstrates the 1-hr fractional myocardial ^{99m}Tc-teboroxime clearances for the control, 30-min and 60-min no flow/reflow groups. Fractional clearances were significantly greater for the 30-min and 60-min no flow/reflow groups (0.65 ± 0.01 and 0.65 ± 0.01, respectively) compared to

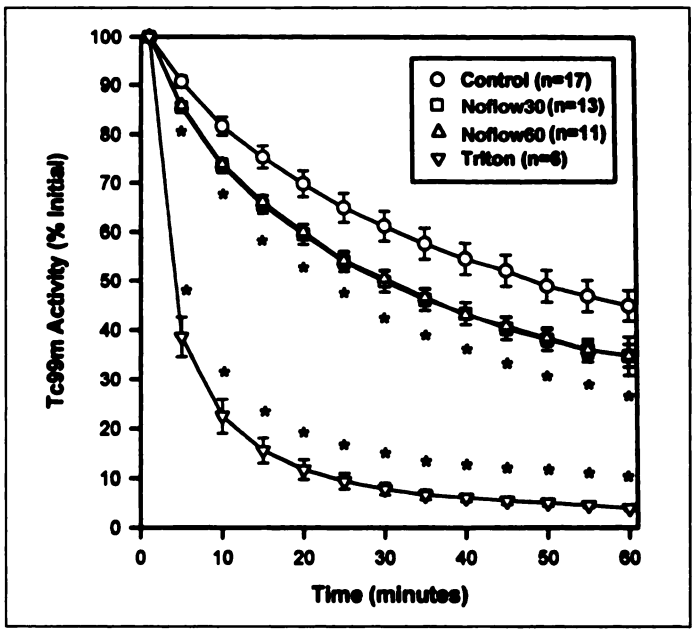

FIGURE 5. Mean decay and background-corrected ^{99m}Tc-teboroxime myocardial clearance curves for Control, 30-min no flow/reflow, 60-min no flow/reflow and Triton X-100-treated hearts. *p < 0.01 compared to control.

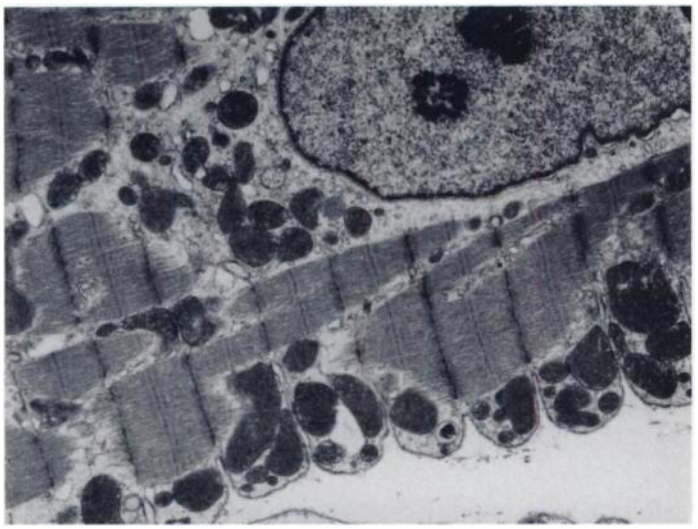

FIGURE 6. Representative electron micrograph from a control heart.

controls (0.55 ± 0.01, p < 0.05). Triton X-100 hearts demonstrated an even greater fractional clearance (0.96 ± 0.01, p < 0.05) compared to the other groups.

Electron Microscopy

Figures 6, 7, 8 and 9 represent electron micrographs from control, 30-min no flow/reflow, 60-min no flow/reflow and Triton X-100 hearts, respectively. Control hearts demonstrated normal appearance of mitochondria and myofibrils (Fig. 6). The few minor abnormalities noted in the control hearts were most likely due to processing of the tissues for observation. The 30-min no flow/reflow hearts demonstrated normal appearance in most areas as shown in Figure 7. However, some evidence of injury to mitochondria was demonstrated by swelling of the mitochondrial matrix and presence of relatively small intramitochondrial amorphous densities. Some evidence of cell swelling and bleb formation was also noted. The 60-min no flow/reflow hearts, while having patches of normal-appearing myocardium, had substantially more injured tissue that provided evidence of more severe injury (Fig. 8). Variations in mitochondrial size indicative of swelling were noted along with clearing of the mitochondrial matrix. Large electron-dense inclusions were present in many mitochondria. Disruptions in the sarcoplasmic reticulum were observed along with irregular Z bands in some areas. Triton X-100 hearts demonstrated

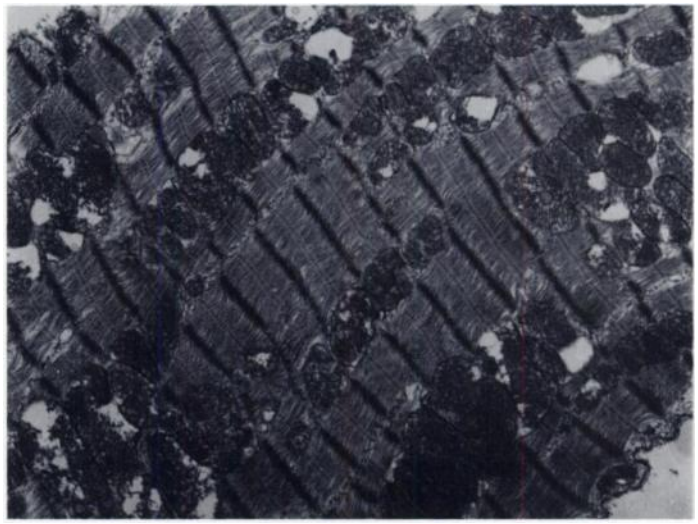

FIGURE 7. Representative electron micrograph from a 30-min no flow/reflow heart.

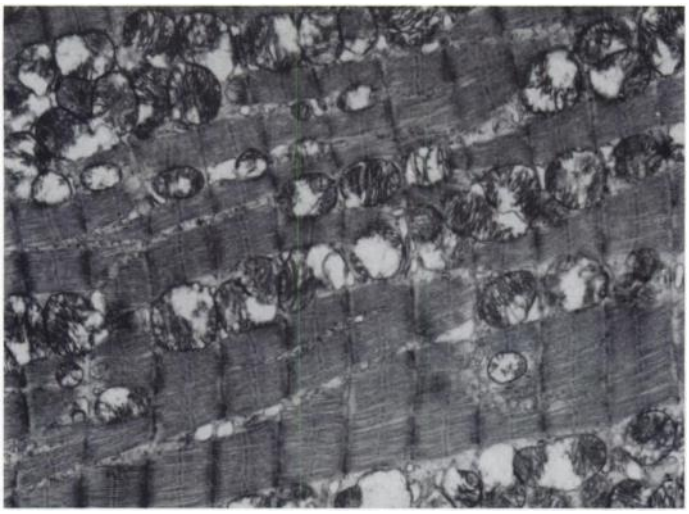

FIGURE 8. Representative electron micrograph from a 60-min no flow/reflow heart.

extensive alterations as seen in Figure 9. Many mitochondria demonstrated marked disruption, reduced numbers or absence of cristae and a lucent matrix. Large amorphous densities were often observed as were irregular Z bands. The most significant changes were the severe sarcolemmal and mitochondrial disruption. These alterations to cell membranes and mitochondria were consistent with severe irreversible cell injury.

DISCUSSION

Technetium-99m-Teboroxime Uptake

Technetium-99m-teboroxime has been shown to be taken up by viable myocardium with uptake related to blood flow (*2,3,12*). Leppo and associates have shown that peak ^{99m}Tc-teboroxime extraction determined by paired indicator dilution technique also correlated with blood flow (*13*). However, the kinetics of ^{99m}Tc-teboroxime uptake in normal and nonviable myocardium have not been well studied.

The current study demonstrated that ^{99m}Tc-teboroxime myocardial uptake was taken up with a nearly linear shape and an uptake curve index near unity for control and 30-min no flow/reflow hearts. However, the more severely injured 60-min no flow/reflow hearts demonstrated curvilinear uptake with a significantly reduced curve index compared to the other two groups. This would suggest a normal volume of distribution in the mildly injured group and a reduced volume of distribution in the severely injured group. The first 5 min of uptake were analyzed separately, since it was felt that this portion of the curve was most relevant to bolus administration in patients. This analysis also demonstrated reduced uptake in the Noflow60 group compared to both control and Noflow30 groups.

FIGURE 9. Representative electron micrograph from a Triton X-100-treated heart.

Regarding myocardial uptake kinetics, Maublant et al. (*14*) have reported an uptake half-time of less than 2 min for ^{99m}Tc-teboroxime in cultures of normal-beating newborn rat myocardial cells. Smith et al. (*4*) fitted ^{99m}Tc-teboroxime time-activity uptake curves from a canine coronary occlusion model to a two-compartment, first-order kinetics model. They found that the washin parameter k21 decreased significantly when flow decreased. Abraham et al. (*15*) used a 60-min occlusion followed by reperfusion swine model and found that infarct/normal zone ^{99m}Tc-teboroxime ratios were lower than corresponding blood flow ratios after 60 min of reperfusion. They concluded that ^{99m}Tc-teboroxime requires viable myocardium for retention and is not exclusively a tracer of blood flow when imaged 5–7 min after injection.

The effects of metabolic factors on ^{99m}Tc-teboroxime myocardial uptake has been studied in monolayers of contractile heart cells. Kronauge et al. (*16*) found that incubation with cationic membrane transport inhibitors had little effect on uptake; however, metabolic inhibitors had a modest influence. Maublant et al. (*17*) found that ^{99m}Tc-teboroxime uptake was decreased at low temperature, while metabolic inhibition had no effect. They also found that osmotic cell lysis had no definite effect on tracer uptake. This is somewhat in contrast to the current study that demonstrates markedly reduced ^{99m}Tc-teboroxime retention after Triton X-100, a membrane detergent. However, the differences between these two studies include the facts that the Maublant model had no flow during the entire study and that osmotic lysis does leave myocardial membrane fragments intact.

Myocardial Clearance

The current study demonstrates that normal myocardium has a biexponential ^{99m}Tc-teboroxime clearance curve with a fast followed by slow component. This is in agreement with previous reports (*1,16*). Previously, however, the clearance kinetics in reperfused infarcted myocardium have not been well studied. In the current study, we found that mildly and severely injured myocardium demonstrates biexponential and increased 60-min fractional clearance compared to controls. The faster clearance was found to be due to the differences in the late slow component rather than the early fast clearance component. Pieri et al. have reported slightly faster clearance from myocardium subjected to 45 min of coronary occlusion followed by 30–45 min of reperfusion (*12*). However, the presence or absence of infarction was not mentioned.

Differential myocardial ^{99m}Tc-teboroxime clearance kinetics previously have been reported in noninfarcted viable tissue. Myocardial clearance from noninfarcted viable tissue is related to blood flow and is increased with higher than normal flow rates and decreased with lower than normal flow rates (*3,5,6,9,10,18*). This change in clearance rate has been attributed to changes in the early $t_{1/2}$ by some investigators (*7*) and to changes in the late $t_{1/2}$ by others (*1*). The change in clearance rate in low flow states has been shown to be due to a combination of hypoxia and reduced flow per se (*8*).

This study demonstrates markedly accelerated ^{99m}Tc-teboroxime clearance after exposure to Triton X-100, a membrane detergent. This agent induced a rapid and irreversible severe injury to sarcolemmal and organelle membranes. Thus,

^{99m}Tc-teboroxime retention appears to be highly dependent upon sarcolemmal integrity.

Potential Study Limitations

The current study used Krebs-Henseleit buffer perfusion. Dahlberg et al. (*19*) and Rumsey et al. (*20*) have shown that ^{99m}Tc-teboroxime binds to blood components. This binding causes reduced ^{99m}Tc-teboroxime extraction and increases the apparent rate of overall cardiac clearance. In pilot studies, we have also observed faster overall clearance in red blood cell perfused hearts. Furthermore, the faster clearance from infarcted reperfused myocardium compared to controls is again observed.

CONCLUSION

Normal and mildly injured reperfused myocardium demonstrates near linear and rapid ^{99m}Tc-teboroxime uptake with a curve index near unity. Severely injured reperfused myocardium demonstrates a curvilinear uptake, with a reduced curve index. Myocardial ^{99m}Tc-teboroxime clearance is biexponential from infarcted reperfused myocardium, with significantly shorter late $t_{1/2}$ in infarcted reperfused myocardium compared to normal. This results in significant increases in 60-min fractional clearance in infarcted reperfused myocardium. Technetium-99m-teboroxime myocardial clearance is greatly accelerated after Triton X-100, indicating that ^{99m}Tc-teboroxime retention is highly dependent upon sarcolemmal integrity.

ACKNOWLEDGMENTS

We thank Dr. William Eckelman and Squibb Diagnostics for their continued support of this investigation and Andrea Lightfoot for her excellent administrative assistance. This study is dedicated to the William K. Warren Family and Foundation for their continued support of medical research.

REFERENCES

1. Stewart RE, Schwaiger M, Hutchins GD, et al. Myocardial clearance kinetics of technetium-99m-SQ30217: a marker of regional myocardial blood flow. *J Nucl Med* 1990;31:1183–1190.
2. Di Rocco RJ, Rumsey WL, Kuczynski BL, Linder KE, Pirro JP, Narra RK, Nunn AD. Measurement of myocardial blood flow using a co-injection technique for technetium-99m-teboroxime, technetium-96-sestamibi and thallium-201. *J Nucl Med* 1992;33: 1152–1159.
3. Beanlands R, Muzik O, Nguyen N, Petry N, Schwaiger M. The relationship between myocardial retention of technetium-99m-teboroxime and myocardial blood flow. *J Am Coll Cardiol* 1992;20:712–719.
4. Smith AM, Gullberg GT, Christian PE, Datz FL. Kinetic modeling of teboroxime using dynamic SPECT imaging of a canine model. *J Nucl Med* 1994;35:484–495.
5. Stewart RE, Heyl B, O'Rourke RA, Blumhardt R, Miller DD. Demonstration of differential post-stenotic myocardial technetium-99m-teboroxime clearance kinetics after experimental ischemia and hyperemic stress. *J Nucl Med* 1991;32:2000–2008.
6. Gray WA, Gewirtz H. Comparison of ^{99m}Tc-teboroxime with thallium for myocardial imaging in the presence of a coronary artery stenosis. *Circulation* 1991;84:1796–1807.
7. Johnson G, Glover DK, Hebert CB, Okada RD. Early myocardial clearance kinetics of technetium-99m-teboroxime differentiate normal and flow-restricted canine myocardium at rest. *J Nucl Med* 1993;34:630–636.
8. Johnson G, Okada RD, Glover DK, Hebert CB. A combination of hypoxia and low flow reduce myocardial CardioTec clearance in ischemic myocardium. In: Schmidt HAE, Hofer R, eds. *Nuclear medicine: nuclear medicine in research and practice*. Vienna: Schattauer; 1991:171–174.
9. Johnson G, Glover DK, Hebert CB, Okada RD. Myocardial technetium-99m-labeled teboroxime clearance derived from canine scans differentiates severity of stenosis after dipyridamole. *J Nucl Cardiol* 1994;1:338–350.
10. Johnson G, Glover DK, Hebert CB, Okada RD. Myocardial clearance kinetics of Tc-99m-teboroxime following dipyridamole: differentiation of stenosis severity in canine myocardium. *J Nucl Med* 1995;36:111–119.
11. Heller LI, Villegas BJ, Weiner BH, McSherry BA, Dalhberg ST, Leppo JA. Use of sequential teboroxime imaging for the detection of coronary artery occlusion and reperfusion in ischemic and infarcted myocardium. *Am Heart J* 1994;127:779–785.
12. Pieri P, Yasuda T, Fischman AJ, Ahmad M, Moore R, Yaoita H, Strauss HW. Myocardial accumulation and clearance of technetium-99m-teboroxime at 100%, 75%, 50% and zero coronary blood flow in dogs. *Eur J Nucl Med* 1991;18:725–731.
13. Leppo JA, Meerdink DJ. Comparative myocardial extraction of two technetium-labeled BATO derivatives (SQ30217, SQ32014) and thallium. *J Nucl Med* 1990;31: 67–74.
14. Maublant JC, Moins N, Gachon P. Uptake and release of two new Tc-99m-labeled myocardial blood flow imaging agents in cultured cardiac cells. *Eur J Nucl Med* 1989;15:180–182.
15. Abraham SA, Mirecki FN, Levine D, Nunn A, Strauss HW, Gewirtz H. Myocardial technetium-99m-teboroxime activity in acute coronary artery occlusion and reperfusion: relation to myocardial blood flow and viability. *J Nucl Med* 1995;36:1062–1068.
16. Kronauge JF, Chiu ML, Cone JS, Davison A, Holman BL, Jones AG, Piwnica-Worms D. Comparison of neutral and cationic myocardial perfusion agents: characteristics of accumulation in cultured cells. *Nucl Med Biol* 1992;19:141–148.
17. Maublant JC, Moins N, Gachon P, Renoux M, Zhang Z, Veyre A. Uptake of technetium-99m-teboroxime in cultured myocardial cells: comparison with thallium-201 and technetium-99m-sestamibi. *J Nucl Med* 1993;34:255–259.
18. Marshall RC, Leidholdt EM, Zhang D-Y, Barnett CA. The effect of flow on technetium-99m-teboroxime (SQ30217) and thallium-201 extraction and retention in rabbit heart. *J Nucl Med* 1991;32:1979–1988.
19. Dahlberg ST, Gilmore MP, Leppo JA. Interaction of technetium-99m-labeled teboroxime with red blood cells reduces the compound's extraction and increases apparent cardiac washout. *J Nucl Cardiol* 1994;1:270–279.
20. Rumsey WL, Rosenspire KC, Nunn AD. Myocardial extraction of teboroxime: effects of teboroxime interaction with blood. *J Nucl Med* 1992;33:94–101.